

Organocatalyzed Birch Reduction Driven by Visible Light

Authors: Justin P. Cole^{1,3}, Dian-Feng Chen^{1,3}, Max Kudisch¹, Ryan M. Pearson¹, Chern-Hooi Lim², Garret M. Miyake^{1*}

¹Colorado State University, Department of Chemistry, Fort Collins, CO 80523 USA. ²New Iridium Inc. Boulder, CO 80303 USA. ³These authors contributed equally to this work.

*Correspondence to: garret.miyake@colostate.edu

Abstract: The Birch reduction is a powerful synthetic methodology that uses solvated electrons to convert inert arenes to 1,4-cyclohexadienes—valuable intermediates for building molecular complexity. This reaction historically requires dangerous alkali metals and cryogenic liquid ammonia as the solvent, severely limiting application potential and scalability. Here, we introduce benzo[ghi]perylene imides as new organic photoredox catalysts for Birch reductions performed at ambient temperature and driven by visible light. Using low catalyst loadings (<1 mole percent), benzene and other functionalized arenes can be selectively transformed to 1,4-cyclohexadienes in good yields. Mechanistic studies support that this unprecedented visible light induced reactivity is enabled by the ability of the organic photoredox catalyst to harness the energy from two visible light photons to affect a single, high energy chemical transformation, likely proceeding through a solvated electron.

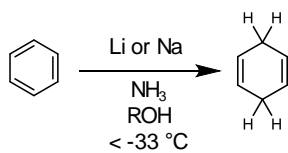
Summary Paragraph:

Generating complex molecules from simple starting materials is an underpinning of synthetic organic chemistry with direct impacts on drug discovery.^{1,2} The Birch reduction is a prime example of such an organic transformation, where a planar aromatic ring is converted to a 1,4-cyclohexadiene with a more complex 3-dimensional structure.³ Birch reductions typically employ alkali metals such as lithium or sodium dissolved in cryogenic liquid ammonia to generate a solvated electron—a powerful reductant which can overcome the stabilization imparted by aromaticity.⁴ The conditions required to perform a traditional Birch reduction are harsh and the reagents are difficult to safely handle making this reaction challenging to perform on a large scale.⁵ Here we report the discovery and application of an organic photoredox catalyst capable of using visible light to reduce benzene and other simple arenes to 1,4-cyclohexadienes at ambient temperature. Mechanistic studies support that this unprecedented visible light induced reactivity is enabled by the ability of the organic photoredox catalyst to harness the energy from two visible light photons to affect a single, high energy chemical transformation, likely proceeding through a solvated electron. This new methodology is attractive because it employs an air-stable organic catalyst, is tolerant of a wide range of functional groups, and can be performed on the gram scale using inexpensive commercially available LEDs.

Main Text:

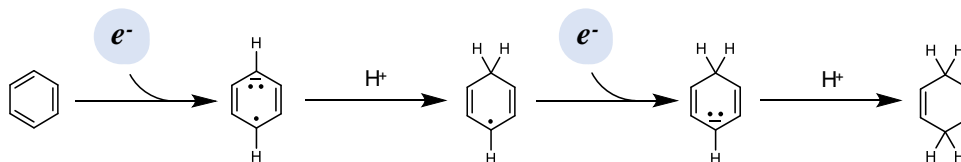
Visible light photoredox catalysis has transformed the synthesis of small molecules and materials through the conversion of photochemical energy to chemical potentials enabling unique reactivity under mild conditions.⁶ However, the scope of accessible chemical transformations using these catalytic platforms is fundamentally confined by the energetics of a visible photon. For example, a 400 nm photon provides 3.1 eV of energy, defining the upper limit for the thermodynamic driving force for transformations using visible light. Thus, the low electron affinity of inert substrates such as benzene render it unreactive and difficult to reduce by single electron transfer requiring a reduction potential of -3.46 V vs SCE,⁷ while the high triplet energy of benzene (3.6 eV) prevents triplet energy sensitization.⁸ As such, the reduction of benzene requires harsher conditions than accessible by current visible light photoredox catalyst systems. The Birch reduction—the prototypical example being the overall $2e^-/2H^+$ reduction of benzene to 1,4-cyclohexadiene—represents one of the most demanding reductions in organic synthesis and employs solvated electrons as the reductant, generated using lithium or sodium metal under cryogenic liquid ammonia conditions (Fig. 1a-b).^{3,9} These dangerous and operationally complex reaction conditions pose severe challenges for both safety and scalability.⁵ Electrochemical^{10,11} and photochemical¹² conditions for Birch reductions have been developed but they require specialized apparatus or intense UV light which can decompose many functional groups and initiate undesirable side reactivity. Thus, the development of a mild, visible light driven Birch reduction would have significant impacts in improving the practicality and scalability of this powerful reaction and ultimately enable broader development of this reaction platform.

a Classic Birch Reduction



- Reduction of inert substrates
- Molecular complexity from simple starting materials
- Dangerous reagents
- Challenging reaction conditions

b Mechanism of Birch Reduction



c Consecutive Photoinduced Electron Transfer (ConPET)

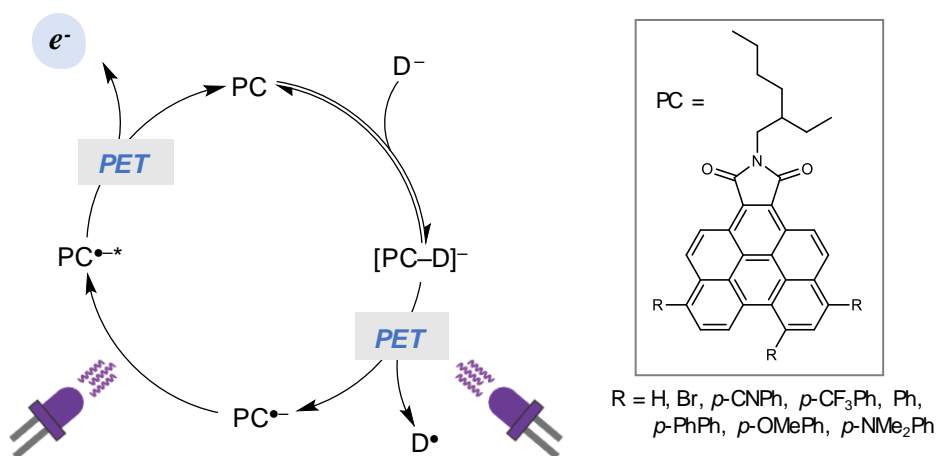


Fig. 1. Background and proposed mechanism of a visible light driven Birch reduction. (a) Reaction conditions and considerations for traditional Birch reduction. **(b)** Mechanism of $2e^-/2\text{H}^+$ reduction of benzene to afford 1,4-cyclohexadiene. **(c)** Mechanism of consecutive photoinduced electron transfer (ConPET) to merge the energetics of two photons to generate a highly reducing solvated electron.

To overcome the energetic constraints of a visible light photon, approaches to harness the energetics of two photons into a single chemical event and access more challenging reactivity have been developed.¹³ For example, under high photon flux conditions using a laser, an iridium (III) complex underwent two successive photoexcitations allowing ionization to iridium (IV) and a solvated electron;¹⁴ while promising, the practicality and utility of this system for Birch reductions remains unknown. Efforts toward a Birch reduction driven by visible light utilized an iridium complex that served as both a triplet sensitizer of the arene as well as a photoreductant in conjunction with a sacrificial electron donor.¹⁵ However, due to the extremely high triplet energy of benzene, triplet sensitization was unsuccessful, and the reduction of benzene was not achieved with reactivity restricted to arenes possessing lower triplet energy. In another approach to accessing more reducing power, the concept of consecutive photoinduced electron transfer (ConPET) was applied with a perylene diimide (PDI) system.¹⁶ Here, the first photon generates an excited-state PDI that is reduced by a sacrificial electron donor to yield a radical anion. Subsequently, the radical anion is photoexcited by a second photon to generate a much stronger reducing species that was employed in the reduction of aryl halides to generate aryl radicals that

could be coupled with an appropriate trapping agent. However, reduction of the aromatic ring was not observed.

Recently, replacing the first photoinduced electron transfer (PET) step to generate the radical anion, electrochemical reduction of naphthalene imides¹⁷ or dicyanoanthracene¹⁸ catalysts were reported. Electrochemical reduction of the catalyst afforded a stable radical anion that can be subsequently photoexcited to a strongly reducing species capable of reducing aryl halides, including aryl chlorides, to aryl radicals for subsequent coupling reactions. Although these systems generate catalyst species with reactivity near Li^0 and excited-state reduction potentials < -3 V vs SCE, reduction of the arene ring was not observed. Thus, Birch reduction reactivity by a visible light photoredox catalyst (PC) system remains elusive.

Our interest in photoredox catalysis originated with the motivation to develop strongly reducing organic PCs for organocatalyzed atom transfer radical polymerization (O-ATRP). Using computationally accelerated discovery we have identified *N,N*-diaryl dihydrophenazines,¹⁹ *N*-aryl phenoxazines,²⁰ and *N*-aryl dimethyl-dihydroacridines²¹ as classes of strongly reducing organic PCs. The most successful O-ATRP catalysts have impressively strong excited-state reduction potentials, some possessing $E^0(\text{PC}^{*+}/\text{PC}^*) < -2$ V vs SCE, representing some of the strongest single visible light photon PC reductants known. This work has motivated us to identify even more strongly reducing PC systems targeting the reduction of benzene and other arenes. Acknowledging the limitations of single photon photoredox catalysis, we envisioned that through exploiting a ConPET process we could realize a catalyst system for the reduction of benzene (Fig. 1c). Our pursuit of a visible light photoredox catalyzed Birch reduction led to the investigation of benzo[ghi]perylene monoimides (BPIs) as potential PCs.²² This class of molecules possesses a computationally predicted high-energy lowest unoccupied molecular orbital (LUMO) [or in equivalence, relatively low electron affinity at $E^0_{\text{comp}}(\text{PC}/\text{PC}^*) \sim -1.3$ V vs. SCE],²³ and we hypothesized the photoexcitation of PC^* to PC^{*+} would prove successful in ConPET for the reduction of benzene. To test this hypothesis, we synthesized a family of targeted PCs in two to four steps from commercial reagents, resulting in a series of BPI molecules possessing electron neutral, withdrawing, and donating core-substituents on the 6-, 8-, and 11- core-positions of the BPI (Fig. 1c). All these molecules exhibited strong visible light absorption (wavelength of maximum absorption $\lambda_{\text{max}} > 400$ nm and molar absorptivity $\epsilon_{\text{max}} > 20,000$ $\text{M}^{-1}\text{cm}^{-1}$), high-lying LUMOs [$E_{1/2,\text{exp}}(\text{PC}/\text{PC}^*) < -1.2$ V vs. SCE], and redox reversibility for single electron transfers as determined by cyclic voltammetry (Table S5).

To investigate the ability of these molecules to serve as PCs in a ConPET mechanism, we first examined the light-induced reduction of the BPI by an electron donor to generate the PC radical anion (PC^*). Although commonly employed trialkyl amine donors were unreactive with the BPIs, OH^- and F^- proved effective at reducing the BPI under visible light irradiation. Our initial survey of the targeted photoredox catalyzed Birch reduction implemented 2-phenylethanol as the substrate to produce the cyclohexadiene product, 2-(cyclohexa-1,4-dien-1-yl)ethan-1-ol (**1**). Gratifyingly, using the various BPI PCs (0.25 mol%), NBu_4OH (2 equivalents) as the electron source, in mixed methanol and *tert*-amyl alcohol as the solvent and H^+ source, and irradiated with a 405 nm LED resulted in conversion of the arene to the target product, albeit in low conversions (Table S2). The BPI derivative possessing *p*-OMePh core-substituents outperformed the other PCs, resulting in 17% conversion after 16 hours. Surveying potential reductants revealed that using the less sterically hindered NMe_4OH and increasing the loading to 10 equivalents resulted in an increase in conversion to 42% after 48 hours.

The reaction still proceeded using a lower catalyst loading (0.1 mol%), but conversion was not improved with increased catalyst loading (e.g. 1 mol%), presumably because of quenching of the photoexcited PC (PC*) or the catalyst decomposing as an aromatic substrate in the reaction (Table S2). Excitingly, it was found that 88% conversion (70% isolated yield, **1** in Fig. 2b) could be achieved by adding a total of 0.75 mol% of catalyst divided over three additions during the course of the reaction (96 h). Control experiments revealed that the reaction did not proceed or resulted in minimal conversion with omission of any single component (PC, OH⁻, H⁺ source, or light). While the reaction was not oxygen tolerant (PC* can be quenched by O₂, $E^0(\text{O}_2/\text{O}_2^{\bullet-}) \sim -1.0$ V vs SCE) it was tolerant to water.

With these reaction conditions established, we explored the general applicability of this photoinduced Birch reduction (Fig. 2). The reduction of structurally similar 1-phenyl-2-propanol (a secondary alcohol) also proceeded well to afford product **2** in 62% yield. Notably, additional substituents on the phenyl ring affected reaction efficiency. For example, *meta*- and *para*-methyl phenyl ethanol exhibited reduced reactivity and products **3** and **4** were isolated in 51% and 48% yield, respectively. The introduction of a methyl group at the *ortho*-position significantly inhibited the reactivity (**5**, 24% yield). Functional groups, such as carboxylic acid (**6** and **7**), amide (**8**), carbamate (**9** and **10**), and strained cyclopropane (**7**) are well-tolerated. The reduction of feedstocks benzene, toluene, and other simple mono- or di-substituted alkyl benzene derivatives were successful as well, affording **11-14** in moderate to high yields (38-80%). Remarkably, the cyclic ether motif was preserved in the high-yielding reduction of isochroman derivatives (**15** and **16**), while exclusive benzyl C-O bond cleavage occurs under conventional Birch conditions using lithium.²⁴ Similarly, 1,3-dihydroisobenzofuran and 1,2,3,4-tetrahydroisoquinoline were transformed to **17** and **18** in 82% and 40% yield, respectively. We also demonstrated that this Birch reduction method could be scaled up by performing it at 10 mmol (1.2 g) scale, which reached 70% conversion (52% isolated yield, **1** in Fig. 2b) using the same reactant stoichiometry in a larger vessel with 3 additional 405 nm LEDs. Under these prescribed reaction conditions this methodology proved less successful or ineffective in the reduction of electron rich arenes as well as with substrates possessing alkenes, alkynes, alkyl halides, unprotected amines, or nitrogen containing heterocycles (Fig. S1).

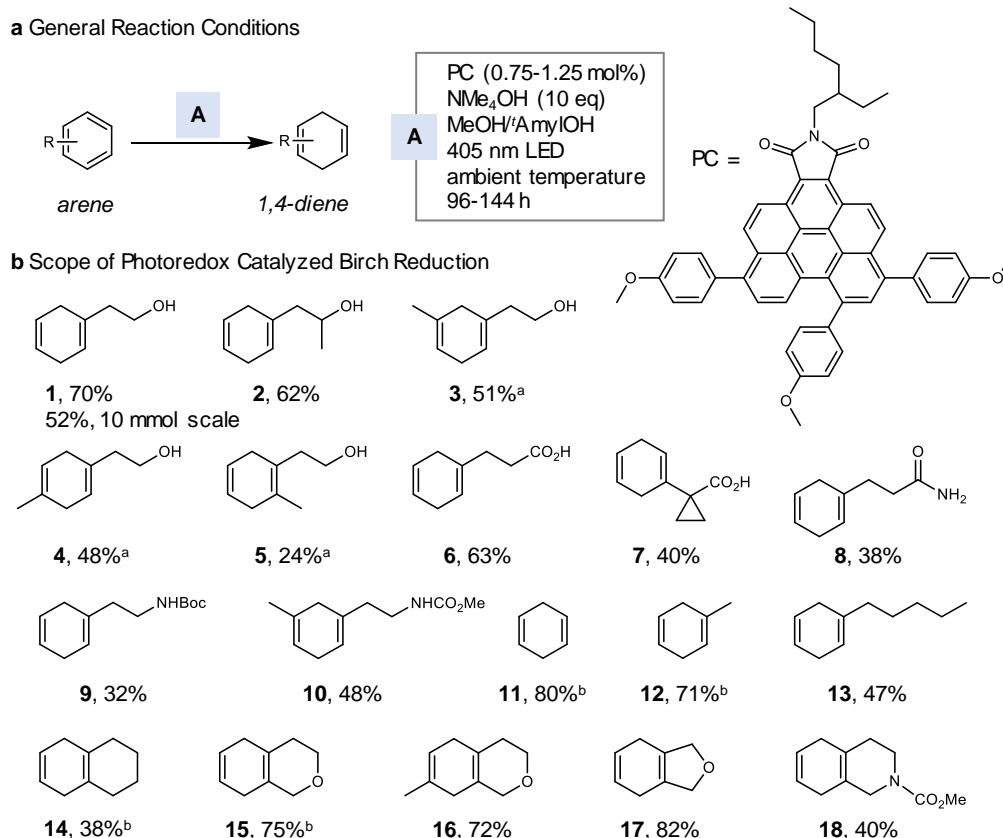
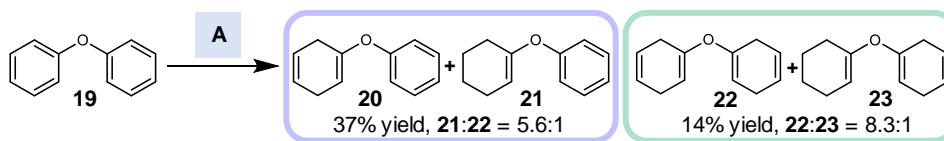


Fig. 2. Synthesis of 1,4-cyclohexadienes by visible light driven Birch reduction of arenes. (a) General reaction conditions. **(b)** Substrate scope; isolated yields are reported unless otherwise indicated. ^a144 h reaction, otherwise 96 h. ^bYield determined by ¹H NMR using 1,3,5-trimethoxybenzene as the internal standard.

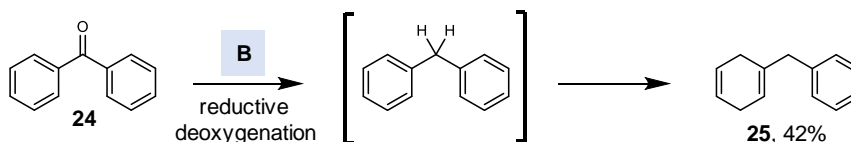
Selective reduction of arenes containing multiple reactive unsaturated functional groups could be achieved through modulation of the reaction conditions (Fig. 3). Interestingly, reduction of one or both phenyl rings of diphenyl ether was observed (**28** and **22**), as well as the over-reduction to afford vinyl ethers **21** and **23**. Employing optimized conditions, benzophenone proceeded through the tandem reductive deoxygenation and Birch reduction to afford 1-benzyl-1,4-cyclohexadiene **25** in 42% yield. By manipulating the equivalents of NMe₄OH and reaction time, cinnamyl alcohol could be converted to either phenylpropanol **27** through alkene reduction or **28** via both alkene and aromatic reductions. Similarly, *trans*-2-phenylcyclopropane-1-carboxylic acid underwent a reductive ring-opening process to give **30** in 73% yield, while further reduction provided **31** in 40% yield. Additionally, dehalogenation of the pharmaceutical loratadine was facile (**33**, 65% yield), although significant transesterification also occurred with the solvent (**34**).

a Reduction of Aryl Ethers



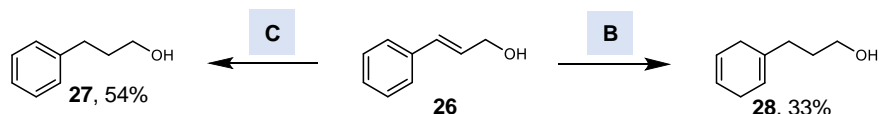
A PC (0.25 mol% x 6), NMe₄OH (5 eq x 3), MeOH/AmyIOH, 405 nm, rt, 168 h

b Reductive Deoxygenation and Birch Reduction



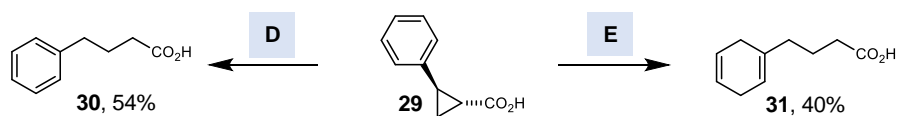
B PC (0.25 mol% x 3), NMe₄OH (5 eq x 3), MeOH/AmyIOH, 405 nm, rt, 96 h

c Selective Reduction



C PC (0.25 mol%), NMe₄OH (5 eq), MeOH/AmyIOH, 405 nm, rt, 24 h

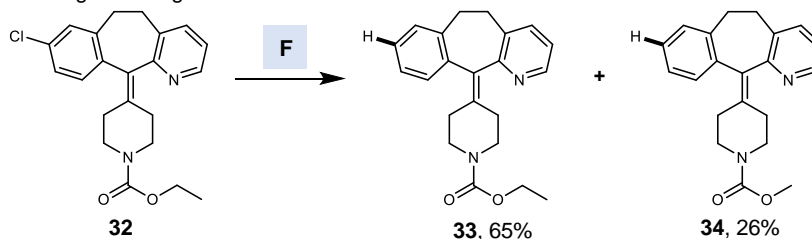
d Selective Reductive Ring-Opening or Birch Reduction



D PC (0.25 mol% x 2), NMe₄OH (10 eq), MeOH/AmyIOH, 405 nm, rt, 72 h

E PC (0.25 mol% x 5), NMe₄OH (15 eq), MeOH/AmyIOH, 405 nm, rt, 144 h

e Late-Stage Dehalogenation



F PC (0.25 mol%), NMe₄OH (10 eq), MeOH/AmyIOH/THF, 405 nm, rt, 48 h

Fig. 3. Selective reductions. Modulation of the reaction conditions enables selective reduction.

To investigate the mechanism underlying this reactivity, a combination of spectroscopic studies and density functional theory (DFT) calculations were performed (Fig. 4). Overall, these results support a ConPET mechanism in this photoredox catalyzed Birch reduction (Fig. 4a). Prior to light absorption, both the absorption and fluorescence spectra of PC were found to blue-shift with OH⁻ addition, confirming interaction between the ground state PC and OH⁻ (Fig. 4b). Observing the UV-visible spectrum during titration with increasing molar ratios of OH⁻ relative to PC show a decrease in PC absorption bands with increasing [OH⁻] in conjunction with the

appearance of new absorbance features ($\lambda_{\text{abs,max}} = 312$ and 412 nm). Monitoring fluorescence of these same mixtures shows a diminishing of the PC fluorescence ($\lambda_{\text{em,max}} = 563$ nm) with the appearance of emission from a new species ($\lambda_{\text{em,max}} = 481$ nm), supporting assignment of a 1:1 equilibrium binding model. Fitting the UV-vis data to this 1:1 model²⁵ yields the equilibrium constant for OH^- association ($K_{\text{eq}} = 920 \text{ M}^{-1}$). It is relevant to note that in the formation of a charge-transfer anion- π complex between iodide and naphthalene diimides (NDIs) a red-shift was noticed, as opposed to the blue-shift observed here, suggesting a fundamentally different complexation between PC and OH^- .²⁶ Interestingly, ^{13}C NMR supports formation of a covalent Meisenheimer-like complex $[\text{PC-OH}]^-$ (Fig. 4b).²⁷ A new signal emerges after the addition of either OH^- ($\delta = 173.9$ ppm) or F^- ($\delta = 173.0$ ppm), which we assign as the quaternary carbon that is formed after nucleophilic attack on the imide moiety by these nucleophiles. Formation of $[\text{PC-OH}]^-$ is further supported by DFT calculations (Fig. 4a), which predicts the complex formation to be exergonic by 3.0 kcal/mol ($K_{\text{eq,comp}} = 149 \text{ M}^{-1}$) along with a qualitative blue-shift in the predicted lowest energy UV-vis absorption ($\lambda_{\text{abs,max}}$ from 408 to 376 nm). The $[\text{PC-OH}]^-$ is stable in the dark such that thermally-induced electron transfer within the complex does not occur and is predicted to be endergonic by 44.8 kcal/mol, although such ground state reactivity was observed with the structurally related PDIs and NDIs.^{28,29}

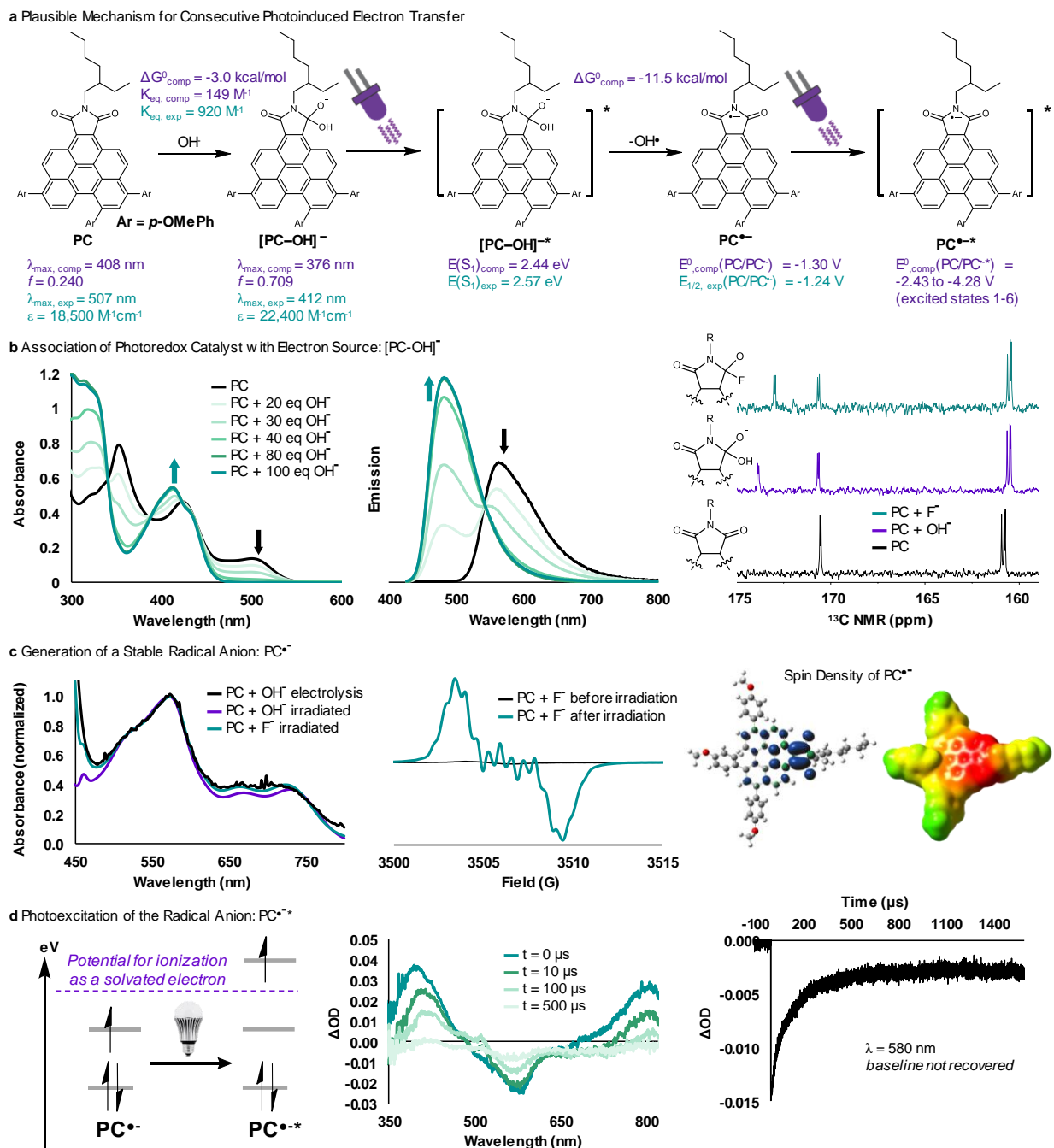


Fig. 4. Mechanistic studies. (a) Proposed mechanism of ConPET proceeds through a covalent [PC-OH]⁻ complex; DFT predicted values are shown in purple and experimentally measured values in turquoise; Electrochemical reference in V vs. SCE; Ar = *p*-OMePh. (b) Association of the PC and OH⁻ can be observed by absorption (left), fluorescence (middle), and ¹³C NMR (right) spectroscopy; R = 2-ethylhexyl (c) The PC•⁻ is stable and can be observed by absorption (left) and EPR (middle) spectroscopy; Computational characterization of PC•⁻ by visualization of spin density and electrostatic potential (ESP)-mapped electron density depicting electron-rich “red” and electron-poor “green” regions (right). (d) Nanosecond transient absorption spectroscopy of PC•⁻; irradiation performed with a 405 nm LED (middle and right).

With the dark speciation and resting state of the PC/OH⁻ complex posited to be [PC-OH]⁻, we next investigated its reactivity under the influence of light (Fig. 4c). Upon photon absorption, we propose that PET occurs intramolecularly from OH⁻ to the imide moiety to form the radical anion PC^{•-} and OH[•], with OH[•] likely being quenched by solvent. This PET step is predicted to be exergonic by 11.5 kcal/mol and thermodynamically driven by the lowest singlet excited state of the [PC-OH]⁻ [$E(S1)_{\text{exp}} = 2.57$ eV; $E(S1)_{\text{comp}} = 2.44$ eV] (Fig. 4a). The formation of PC^{•-} is further supported by various independent experiments. First, upon irradiation of [PC-OH]⁻ with a 405 nm LED a new species is observed ($\lambda_{\text{abs,max}} = 580$ nm) as evidenced by a color change from pale yellow to purple. In support that this new species is the stable PC^{•-}, the same absorbance spectrum could be observed when using F⁻ as the electron source or through bulk electrolysis at an applied potential ($E_{\text{app}} = -2.26$ V vs SCE) (Fig. 4c). Electron paramagnetic resonance (EPR) spectroscopy was used to characterize the photogenerated PC^{•-}. The experimental EPR spectrum could be reasonably simulated with EasySpin software³⁰ and demonstrated delocalization of the unpaired electron on the benzo[ghi]perylene monoimide core as indicated by its interactions with N ($a = 1.985$ G), two equivalent methylene Hs adjacent to the N ($a = 0.540$ G), and seven non-degenerate Hs on the aromatic core (a values = 0.611, 0.612, 0.639, 0.644, 0.644, 0.645, and 0.645 G); other parameters used in the simulation include $g_{\text{isotropic}} = 2.00171$, linewidth = 0.666 G and lineshape = gaussian (Fig. S41). PC^{•-} was further characterized by visualization of the DFT-predicted spin density and of the unpaired electron located on the imide moiety and to a lesser extent delocalizing over the methylene group adjacent to nitrogen and the aromatic system on the perylene core.

Although PC^{•-} is a relatively strong reductant [$E_{1/2,\text{exp}}(\text{PC}/\text{PC}^{\bullet-}) = -1.24$ V vs SCE; $E^0_{\text{comp}}(\text{PC}/\text{PC}^{\bullet-}) = -1.30$ V vs SCE], this reducing power is insufficient for a Birch reduction and reactivity is not observed in the absence of light. Thus, we hypothesized that PC^{•-} absorbs a second photon to generate PC^{•-*}, a much stronger reductant that can engage in Birch reduction (Fig. 4d). Notably, PC^{•-} is a persistent radical with sufficient lifetime for reversible CV and EPR analysis. This long-lifetime allows PC^{•-} to absorb a photon using a practical LED setup as opposed to requiring laser irradiation.¹⁴ The excited state properties of the PC^{•-*} were predicted using time-dependent DFT calculations to evaluate the thermodynamic feasibility of generating a solvated electron. We determined that the first six excited states of PC^{•-*} can be accessed with a 405 nm photon (3.06 eV) used in this study (Fig. S113). Excited states 2 through 6 have enough energy for ionization of PC^{•-*} by an electron transfer to the solvent ($k_{\text{ET},1}$) forming a solvated electron and recovering the ground state PC. For efficient generation of a solvated electron, $k_{\text{ET},1}$ must be competitive with the internal conversion process (k_{IC}) deactivating high-lying excited states to the lowest excited state of PC^{•-*}, which is below the energy threshold for solvated electron formation. Further, electron transfer to an aromatic substrate ($k_{\text{ET},2}$) for Birch reduction reactivity must also be facile relative to the unproductive back electron transfer to the lowest excited state of PC^{•-*} ($k_{\text{ET},3}$).

The photoexcitation of PC^{•-} was investigated using nanosecond transient absorption spectroscopy (Fig. 4d). Selective excitation of PC^{•-} could be achieved through irradiation at 532 nm due to the minimal spectral overlap with PC or [PC-OH]⁻. Laser excitation produces a ground state bleach feature ($\lambda_{\text{min}} = 580$ nm) that matches the absorption of PC^{•-} and thus can be assigned to PC^{•-*}. Kinetic monitoring of this signal reveals that the baseline is not recovered on the millisecond timescale, indicating that the process does not regenerate PC^{•-} and supporting the possibility of generating a solvated electron. Comparing the kinetic traces when benzene substrate is present as a potential quencher reveals that benzene does not directly quench PC^{•-*}, consistent with the hypothesis that a solvated electron generated upon irradiation of PC^{•-} is responsible for

this reactivity (Fig. S15). Furthermore, control experiments reveal that in the absence of OH⁻, the PC* is not quenched by either benzene or alcohols, supporting that the ConPET mechanism proceeds through [PC-OH]⁻ and enables the Birch reduction reactivity.

In sum, a class of organic benzo[ghi]perylene imide photoredox catalysts were developed for Birch reductions under mild benchtop conditions and visible light LED irradiation. We envision that this photoredox catalyzed system will advance the capabilities of Birch reductions by providing a robust and facile synthetic methodology. Further, by eliminating harsh and dangerous reaction conditions, this system may promote broader implementation of Birch reductions in chemical transformations and we anticipate that the mechanistic concepts presented herein will inspire discovery of novel catalytic systems for exciting and powerful chemical transformations.

References:

- (1) Chen, T.; Barton, L. M.; Lin, Y.; Tsien, J.; Kossler, D.; Bastida, I.; Asai, S.; Bi, C.; Chen, J. S.; Shan, M.; Fang, H.; Fang, F. G.; Choi, H.; Hawkins, L.; Qin, T.; Baran, P. S. Building C(sp³)-Rich Complexity by Combining Cycloaddition and C—C Cross-Coupling Reactions. *Nature* **2018**, *560*, 350-354.
- (2) Lovering, F.; Bikker, J.; Humblet, C. Escape from Flatland: Increasing Saturation as an Approach to Improving Clinical Success. *Journal of Medicinal Chemistry* **2009**, *52*, 6752-6756.
- (3) Birch, A. J. 117. Reduction by dissolving metals. Part I. *Journal of the Chemical Society* **1944**, 430-436.
- (4) Krapcho, A. P.; Bothner, A. A. Kinetics of the Metal-Ammonia-Alcohol Reductions of Benzene and Substituted Benzenes. *Journal of the American Chemical Society* **1959**, *81*, 3658-3666.
- (5) Joshi, D. K.; Sutton, J. W.; Carver, S.; Blanchard, J. P. Experiences with Commercial Production Scale Operation of Dissolving Metal Reduction Using Lithium Metal and Liquid Ammonia. *Organic Process Research & Development* **2005**, *9*, 997-1002.
- (6) Yoon, T., Ischay, M. & Du, J. Visible light photocatalysis as a greener approach to photochemical synthesis. *Nature Chemistry* **2010**, *2*, 527-532.
- (7) Mortensen, J.; Heinze, J. The Electrochemical Reduction of Benzene—First Direct Determination of the Reduction Potential. *Angewandte Chemie International Edition in English* **1984**, *23*, 84-85.
- (8) Ishikawa, H.; Noyes, W. A. The Triplet State of Benzene. *Journal of the American Chemical Society* **1962**, *84*, 1502-1503.
- (9) Birch, A. J. The Birch Reduction in Organic Synthesis. *Pure & Applied Chemistry* **1996**, *68*, 553-556.
- (10) Birch, A. J. Electrolytic Reduction in Liquid Ammonia. *Nature* **1946**, *158*, 60-60.
- (11) Peters, B. K.; Rodriguez, K. X.; Reisberg, S. H.; Beil, S. B.; Hickey, D. P.; Kawamata, Y.; Collins, M.; Starr, J.; Chen, L.; Udyavara, S.; Klunder, K.; Gorey, T. J.; Anderson, S. L.; Neurock, M.; Minter, S. D.; Baran, P. S. Scalable and safe synthetic organic electroreduction inspired by Li-ion battery chemistry. *Science* **2019**, *363*, 838-845.

- (12) Yasuda, M.; Pac, C.; Sakurai, H. Photochemical reactions of aromatic compounds. 35. Photo-Birch reduction of arenes with sodium borohydride in the presence of dicyanobenzene. *The Journal of Organic Chemistry* **1981**, *46*, 788-792.
- (13) Glaser, F.; Kerzig, C.; Wenger, O. S. Multiphoton Excitation in Photoredox Catalysis: Concepts, Applications, Methods. *Angewandte Chemie International Edition* in press DOI: 10.1002/anie.201915762.
- (14) Kerzig, C.; Guo, X.; Wenger, O. S. Unexpected Hydrated Electron Source for Preparative Visible-Light Driven Photoredox Catalysis. *Journal of the American Chemical Society* **2019**, *141*, 2122-2127.
- (15) Chatterjee, A.; König, B. Birch-Type Photoreduction of Arenes and Heteroarenes by Sensitized Electron Transfer. *Angewandte Chemie International Edition in English* **2019**, *58*, 14289-14294.
- (16) Ghosh, I.; Ghosh, T.; Bardagi, J. I.; König, B. Reduction of aryl halides by consecutive visible light-induced electron transfer processes. *Science* **2014**, *346*, 725-728.
- (17) Cowper, N. G. W.; Chernowsky, C. P.; Williams, O. P.; Wickens, Z. K. Potent Reductants via Electron-Primed Photoredox Catalysis: Unlocking Aryl Chlorides for Radical Coupling. *Journal of the American Chemical Society* **2020**, *142*, 2093-2099.
- (18) Kim, H.; Kim, H.; Lambert, T. H.; Lin, S. Reductive Electrophotocatalysis: Merging Electricity and Light To Achieve Extreme Reduction Potentials. *Journal of the American Chemical Society* **2020**, *142*, 2087-2092.
- (19) Theriot, J. C.; Lim, C.-H.; Yang, H.; Ryan, M. D.; Musgrave, C. B.; Miyake, G. M. Organocatalyzed atom transfer radical polymerization driven by visible light. *Science* **2016**, *352*, 1082-1086.
- (20) Pearson, R. M.; Lim, C.-H.; McCarthy, B. G.; Musgrave, C. B.; Miyake, G. M. Organocatalyzed Atom Transfer Radical Polymerization Using N-Aryl Phenoxazines as Photoredox Catalysts. *Journal of the American Chemical Society* **2016**, *138*, 11399-11407.
- (21) Buss, B. L.; Lim, C.-L.; Miyake, G. M. Dimethyl Dihydroacridines as Photocatalysts in Organocatalyzed Atom Transfer Radical Polymerization of Acrylate Monomers. *Angewandte Chemie International Edition* **2020**, *59*, 3209-3217.
- (22) Manning, S. J.; Bogen, W.; Kelly, L. A. Synthesis, Characterization, and Photophysical Study of Fluorescent N-substituted Benzo[ghi]perylene “Swallow Tail” Monoimides. *The Journal of Organic Chemistry* **2011**, *76*, 6007-6013.
- (23) Gerber, L. C. H.; Frischmann, P. D.; Fan, F. Y.; Doris, S. E.; Qu, X.; Scheuermann, A. M.; Persson, K.; Chiang, Y.-M.; Helms, B. A. Three-Dimensional Growth of Li₂S in Lithium–Sulfur Batteries Promoted by a Redox Mediator. *Nano Letters* **2016**, *16*, 549-554.
- (24) Almena, J.; Foubelo, F.; Yus, M. Lithium 2-(2-lithiomethylphenyl)ethanolate from isochroman: Easy preparation of substituted benzoxepines and functionalised arenes. *Tetrahedron* **1995**, *51*, 3365-3374.
- (25) Thordarson, P. Determining association constants from titration experiments in supramolecular chemistry. *Chemical Society Reviews* **2011**, *40*, 1305-1323.
- (26) Guha, S.; Goodson, F. S.; Corson, L. J.; Saha, S. Boundaries of Anion/Naphthalenediimide Interactions: From Anion– π Interactions to Anion-Induced Charge-Transfer and Electron-Transfer Phenomena. *Journal of the American Chemical Society* **2012**, *134*, 13679-13691.
- (27) Dawson, R. E.; Hennig, A.; Weimann, D. P.; Emery, D.; Ravikumar, V.; Montenegro, J.; Takeuchi, T.; Gabutti, S.; Mayor, M.; Mareda, J.; Schalley, C. A.; Matile, S. Experimental

evidence for the functional relevance of anion- π interactions. *Nature Chemistry* **2010**, *2*, 533-538.

(28) Saha, S. Anion-Induced Electron Transfer. *Accounts of Chemical Research* **2018**, *51*, 2225-2236.

(29) Goodson, F. S.; Panda, D. K.; Ray, S.; Mitra, A.; Guha, S.; Saha, S. Tunable electronic interactions between anions and perylenediimide. *Organic & Biomolecular Chemistry* **2013**, *11*, 4797-4803.

(30) Stoll, S.; Schweiger, A. EasySpin, a comprehensive software package for spectral simulation and analysis in EPR. *Journal of Magnetic Resonance* **2006**, *178*, 42-55.

Acknowledgments: This work was supported by Colorado State University and the National Institutes of Health under Award Number R35GM119702. The content is solely the responsibility of the authors and does not necessarily represent the official views of the National Institutes of Health. This work used the Extreme Science and Engineering Discovery Environment (XSEDE), which is supported by National Science Foundation Grant ACI-1548562.

Author Contributions: J.P.C. and G.M.M. conceived the project. J.P.C., D.-F.C., M.K. R.M.P., and C.-H.L. designed and performed the experiments. J.P.C., D.-F.C., M.K. R.M.P., C.-H.L., and G.M.M analyzed the data and prepared the manuscript.

Competing interests: We have filed a provisional patent application on the work described here

Data and materials availability: Single-crystal X-ray diffraction data is deposited at the Cambridge Crystallographic Data Center under CCDC 1912318 and is contained in the .CIF file attached to this manuscript. All data is available in the main text or the supplementary materials

Supplementary Information:

Materials and Methods

Figures S1-S114

Tables S1-S7

Coordinates of Calculated Molecular Structures

X-Ray Crystallographic Data for **PC 8**